

Research Article

The phyto melatonin receptor (PMRT1) *Arabidopsis* Cand2 is not a *bona fide* G protein–coupled melatonin receptor

Hyoung Yool Lee¹, Kyoungwhan Back^{1*}¹Department of Biotechnology, College of Agriculture and Life Sciences, Chonnam National University, Gwangju 61186, Republic of Korea

*Correspondence: kback@chonnam.ac.kr, Tel: +82 62 530 2165

Running title: Functional role of Cand2

Received: March 19, 2020; Accepted: May 28, 2020

ABSTRACT

It was recently suggested that the protein Cand2 acts as a G protein–coupled receptor (GPCR) for melatonin in *Arabidopsis* by mediating stomatal closure via H₂O₂ production and Ca²⁺ influx. Here, we examined whether Cand2 is indeed a melatonin receptor. Contrary to previous reports, confocal microscopy analyses indicated that Cand2 protein is localized in the cytoplasm rather than the plasma membrane. The role of Cand2 was further investigated in genetic analyses using two *Arabidopsis cand2* knockout mutant lines, SALK_071302 (*cand2-1*) and SALK_068848 (*cand2-2*). We found that melatonin-mediated mitogen-activated protein kinase (MAPK) activation was not abolished in the *cand2* mutant lines, nor did melatonin-mediated defense gene induction (e.g., *GST1*) change relative to that in the wild type Col-0. Following ER stress, the two *cand2* mutant lines were identical to Col-0 in terms of defense gene induction, ion leakage, and ROS levels. Two G protein mutants, *gpa1* (G α mutant) and *agb1* (G β mutant), also exhibited no disturbance in melatonin-mediated defense gene induction or melatonin-mediated MAPK activation. Collectively, our data indicate that Cand2 is neither a phyto melatonin receptor localized in the plasma membrane nor is it involved in the melatonin-mediated defense signaling pathway via G protein components. However, it remains unclear how melatonin-mediated MAPK activation was slightly decreased in the mutant *cand2-2* without affecting downstream defense gene induction. Also, it cannot rule out the possibility that Cand2 may be a melatonin binding protein and that its binding may result in a decrease of free melatonin level in plants.

Key words: *Arabidopsis*; Cand2; defense genes; G proteins; GPCR; MAPK; melatonin receptor.

1. INTRODUCTION

In animals, melatonin, known as the ‘hormone of darkness,’ acts via a G protein–coupled receptor (GPCR) signaling pathway. The two melatonin receptors, MT1 and MT2, are located in either the plasma membrane or mitochondria (1, 2). GPCR signaling cascades consist of a receptor and intracellular heterotrimeric G protein complex composed of three subunits: G α , G β , and G γ (Figure 1A). In general, ligand binding to GPCR changes an inactive G α into an active G α by binding GTP, which results in the activation of various downstream effectors for multiple melatonin-mediated responses (3). In contrast, the key G protein, G α , is self-activating in plants, indicating that plant G proteins do not need a GPCR

to activate G α for signaling activation (4). Although many GPCR candidates have been documented in *Arabidopsis* and rice, including GCR1 and candidate GPCR (Cand) proteins, it has since been confirmed that none of these plant GPCR candidates exhibit GPCR activity (5).

Surprisingly, it was recently reported that Cand2 in *Arabidopsis* functions as a melatonin receptor based on melatonin binding assay and melatonin-mediated stomatal closure via H₂O₂ production and Ca²⁺ influx (6). In addition, these authors also reported that Cand2 is expressed in plasma membrane and interacted with G protein α , one of heterotrimeric G proteins. This raises important issues, including whether Cand2 protein is localized in the plasma membrane, and whether it plays a significant role in melatonin-mediated biotic and abiotic resistance in *Arabidopsis*. Here, we addressed these issues to determine whether Cand2 acts as a melatonin receptor in *Arabidopsis*. Based on our data from cytoplasmic localization of Cand2 and melatonin-mediated defense gene induction in *cand2* knockout mutants, we concluded that Cand2 is not G protein-coupled melatonin receptor in plants.

2. MATERIALS AND METHODS

2.1. Plant materials and growth conditions.

Seeds were stratified at 4°C for 3 d, and then sown on a compound soil mixture of vermiculite: peat moss : perlite (1 : 1 : 1). *Arabidopsis* plants were grown under a 14 h light (22°C), 10 h dark (20°C) cycle with 60% humidity and a photon flux density of 50 $\mu\text{mol m}^{-2} \text{s}^{-1}$. Fluorescent light from OSRAM (Seoul, Korea) with 50:50 of 6500K (865 FPL36EX-D) and 4000K (840 FPL36EX-W) was used for light source. The *cand2* knockout mutant lines SALK_071302 (*cand2-1*) and SALK_068848 (*cand2-2*), *gpa1-2* (SALK_066823), and *agb1-1* (CS3976), were obtained from the Arabidopsis Biological Resource Center (ABRC; Ohio State University, Columbus, OH, USA). Tobacco plants (*Nicotiana benthamiana*) were grown under a 14 h light (25°C), 10 h dark (20°C) photoperiod.

2.2. Subcellular localization analyses of AtCand2.

The pER8-mCherry vector and pBIN61-GFP-HA (P35s:GFP-HA) plasmid for the cytoplasmic fluorescence marker (kindly provided by Dr. H.G. Kang, Texas State University, San Marcos, TX, USA) were used in a subcellular localization study of AtCand2. Full-length *AtCand2* cDNA was amplified with PCR using a primer set containing an *AscI* site (forward, 5'-GGG GGC GCG CCA TGC GAG TGC TCA GCG AGA TT-3'; reverse, 5'-GGG GGC GCG CCG TTC CCA ATC AGC GTC GAA GA-3'). Gel-purified PCR products were introduced into the T&A vector (RBC Bioscience, New Taipei City, Taiwan), and the *AscI* inserts of *AtCand2* were ligated into the *AscI* site of the binary vector pER8-mCherry to generate pER8-*AtCand2*-mCherry. Entry clones with full-length FLAGELLIN SENSITIVE2 (*FLS2*) without a stop codon were generated by PCR amplification using primers that contained *attB1* and *attB2* sites (forward, 5'-GGGG ACA AGT TTG TAC AAA AAA GCA GGC TTC ATG AAG TTA CTC TCA AAG ACC TTT TTG ATA-3'; reverse, 5'-GGG GAC CAC TTT GTA CAA GAA AGC TGG GTC AAC TTC TCG ATC CTC GTT A-3'). Gel-purified PCR products were introduced into pDONR221/ZEO (Invitrogen, Carlsbad, CA, USA) using BP-clonase II according to the manufacturer's instructions and transferred to destination vector pEarlyGate103 (P35s-gateway-GFP-His) by recombination using LR-clonase II (Invitrogen). These plasmids were transformed into the *Agrobacterium tumefaciens* strain GV2260 using the freeze-thaw method. Leaves from four-week-old tobacco plants were infiltrated with *Agrobacterium* strains, followed by infiltration with 10 μM β -estradiol

for induction. Images were analyzed using a Leica TCS-SP5 confocal microscope ($\times 63$ oil-immersion objective; Leica, Wetzlar, Germany), then processed using the Leica LAS-AF software version 1.8.2. mCherry was excited with an orange He-Ne laser (594 nm), and emitted light was collected from 576 to 629 nm. GFP fluorescence was induced with a blue argon-ion laser (488 nm), and light emitted between 494 and 546 nm was collected. Individual signals were later superimposed.

2.3. Total RNA isolation and reverse transcription PCR (RT-PCR).

Total RNA was extracted from five-week-old plants using a Nucleospin RNA plant kit (Macherey-Nagel, Duren, Germany). Reverse transcription was performed using a Stratagene reverse transcription kit (Stratagene, La Jolla, CA, USA). The PCR reaction was conducted as following conditions initial denaturation 95°C (3min), denaturation 95°C (30 sec), annealing 56°C (30 sec), and extension 72°C (1 min) with 30 μ l of master mix. The primer sequences for RNA analysis were as follows: *BIP2* (forward, 5'-GCA GGA GGA GAA TCA TCG AC-3'; reverse, 5'-AAA GAG AAC GTC CAG GGA GA-3'); *BIP3* (forward, 5'-GGA GAA GCT TGC GAA GAA GA-3'; reverse, 5'-ATA ACC GGG TCA CAA ACC AA-3'); *CNX1* (forward, 5'-TGG TTT TGG GTT GAA TGT TG-3'; reverse 5'-CTG AAG GGG ATG AAA AAG AAA-3'); *APX1* (forward, 5'-GTG TGT GTC TCC CCG AGA GT-3'; reverse 5'-CTA AGC AGC AAA AGC GCA AC-3'); *GST1* (forward, 5'- GGA CTC ACC AAG CCT GTG TT-3'; reverse 5'-TGA ATC GCA TGA GTT TGA CC-3'); *Cand2* (forward, 5'- GGA GTC ACC GTT CGT GAT TT-3'; reverse 5'-CCA AGA TCG AAA TGC CAA AT-3'); *EF-1a* (EF1ALPHA; At5G60390) was used for signal normalization (forward, 5'-TGG TGA CGC TGG TAT GGT TA-3'; reverse 5'-CAT CAT TTG GCA CCC TTC TT-3').

2.4. Protein extraction and immunoblot analysis of MAPK activation.

Protein extract was prepared with kinase extraction buffer (40 mM HEPES, pH 7.5, 100 mM NaCl, 1 mM EDTA, 10% glycerol, 0.01% Triton X-100, and 1 \times Roche protease inhibitor cocktail) and then centrifuged at 10,000 \times g for 10 min at 4°C. Aliquots of the supernatant were mixed with sample buffer (Tris-HCl, pH 6.8, 10% SDS, 10 mM DTT, 20% glycerol, and 0.05% bromophenol blue). Next, samples were boiled and loaded onto SDS-PAGE gels. Anti-phosphor-44/42 (Erk1/2) antibody (Cell Signaling Technology, Danvers, MA, USA) was incubated overnight at a dilution of 1:2000. Secondary rabbit antibody conjugated with horseradish peroxidase (Roche) was incubated with the membrane for at least 1 h. as described previously (7). Proteins were detected using the ECL system (RPN2132; Amersham Biosciences, Piscataway, NJ, USA).

2.5. Measurement of electrolyte leakage and superoxide staining.

Five-week-old rosette leaves challenged with 1 μ g/mL tunicamycin (Tm, in 0.05% DMSO) were collected and then rinsed briefly with 20 mL water. These leaves were transferred to a 50-mL tube containing 20 mL distilled water. The conductivity of the solution was determined using a conductivity meter (model 1481-61; Cole-Parmer Instrument Company, Vernon Hills, IL, USA) after 10 h incubation at room temperature. Superoxide was detected by staining leaves with nitroblue tetrazolium (NBT) as follows. *Arabidopsis* leaves treated with Tm were detached and placed in a solution containing 0.1% NBT (in 10 mM MES, pH 6.8) for 4 h. Thereafter, the leaves were destained and stored in 96% ethanol as described previously (8).

2.6. Statistical analysis.

Asterisks indicate significantly different values at $P < 0.05$, according to post hoc Tukey's honestly significant difference (HSD) tests. Data are presented as means \pm standard deviation from at least three independent experiments.

3. RESULTS AND DISCUSSION

3.1. Knockout mutant screening of *cand2* in *Arabidopsis*.

Two *cand2* knockout mutant lines from the ABRC were chosen for this study: *cand2-1* (Salk_071302), which has T-DNA inserted in the promoter region and was previously used by Wei et al. (6); and *cand2-2* (Salk_068848), which has T-DNA inserted in the exon 1 region (Figure 1B). After screening homozygous lines, we checked the expression levels of *Cand2* in these two mutant lines. The expression levels of *Cand2* mRNA in the *cand2-1* mutant were comparable to those in the wild type Col-0 when observed many times at many different developmental stages. However, the *cand2-2* mutant exhibited no *Cand2* mRNA expression at all, suggesting that *cand2-2* rather than *cand2-1* was the bona fide *cand2* knockout mutant. Thus, the previous *cand2-1* mutant used by Wei et al. (6) was not the true *cand2* knockout mutant. The apparent phenotypes of the two mutant lines differed significantly: *cand2-2* growth was severely retarded whereas *cand2-1* growth was similar to that of Col-0 (Figure 1D, E). These data indicate that *Cand2* is involved in *Arabidopsis* growth. The mechanism underlying this growth retardation in *cand2* remains unknown.

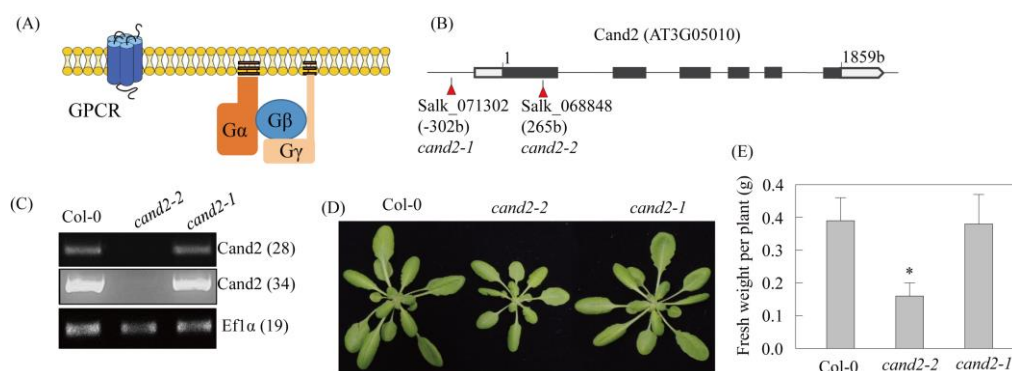


Fig. 1. Schematic diagram of GPCR signaling components and *cand2* mutant analyses.

(A) The components of GPCR signaling pathway. (B) Schematic of T-DNA insertion sites in *Cand2*. (C) *Cand2* transcript levels in the wild type Col-0 and two *cand2* mutants measured by RT-PCR. (D) Soil-grown phenotypes of four-week-old Col-0 and the two independent *cand2* knockout lines, *cand2-1* and *cand2-2*. (E) Shoot weight (FW) of five-week-old Col-0 and *cand2* line plants. Bars show mean fresh weight of six plants \pm SE. Asterisks indicate significant differences from the wild type (Tukey's HSD; $P < 0.05$). GPCR, G protein-coupled receptor.

3.2. Localization of *Cand2* protein by confocal microscopy analyses.

In our localization analysis, we used two marker genes, plasma membrane localized flagellin sensitive2 protein (FLS2) and cytoplasmic green fluorescence protein (GFP), to precisely judge the location of *Cand2* protein expression, because differentiating the cytoplasm from the plasma membrane can be difficult in plant cells due to the larger vacuoles. FLS2 is a Leu-rich repeat transmembrane receptor kinase essential for flagellin

perception localized in the plasma membrane (9). The location of Cand2-mCherry expression was not consistent with that of FLS2-GFP expression, suggesting that Cand2 protein is expressed in subcellular sites other than the plasma membrane (Figure 2). For further confirmation, we compared the Cand2-mCherry expression with the cytoplasmic marker GFP protein (Figure 3). GFP fluorescence matched with Cand2-mCherry expression, indicating cytoplasmic localization of the Cand2 protein.

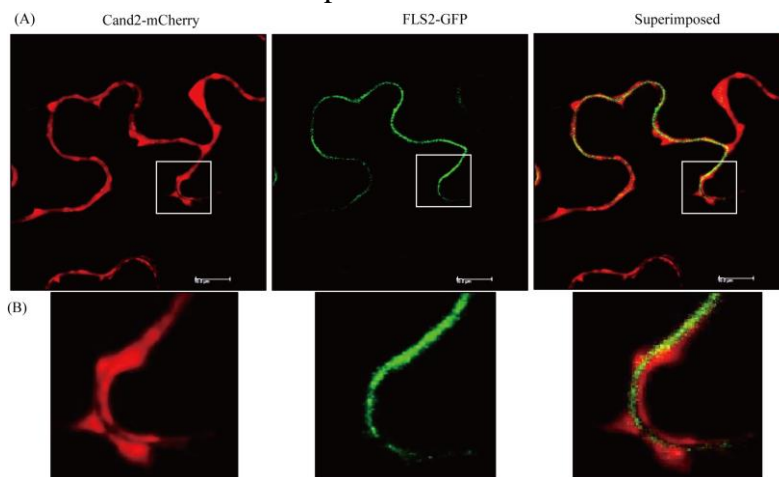


Fig. 2. Localization of Cand2 protein by confocal microscopy analysis.

(A) Subcellular localization of red fluorescence of Cand2-mCherry and green fluorescence of PM-localized FLS2, and superimposed fluorescence images. (B) Magnified images from the boxed region in (A). Left image shows non-PM-localized Cand2-mCherry; middle image shows a PM-localized FLS2-GFP; and right image shows Cand2-mCherry and FLS2-GFP superimposed. Leaves from four-week-old tobacco plants were infiltrated with *Agrobacterium tumefaciens* (GV2260) containing the XVE-inducible Cand2-mCherry or constitutive 35S promoter-driven FLS2-GFP plasmid (plasma membrane marker). Bars = 10 μ m. PM, plasma membrane.

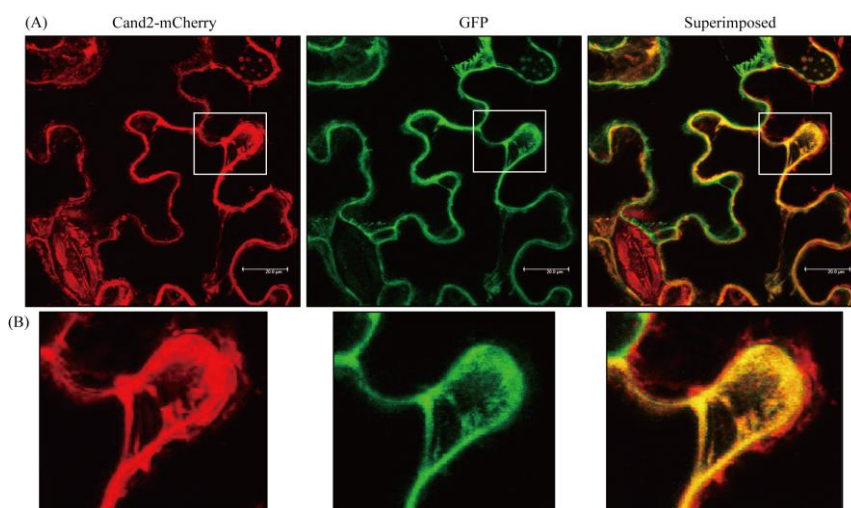


Fig. 3. Localization of Cand2 protein by confocal microscopy analysis.

(A) The red fluorescence of Cand2-mCherry (left) and green fluorescence of cytoplasmic GFP (middle) were viewed separately, and the two fluorescence images were merged (right). (B) Magnified images from the boxed region in (A). Leaves of five-week-old tobacco plants were infiltrated with *Agrobacterium tumefaciens* (GV2260) containing the XVE-inducible Cand2-mCherry or constitutive 35S promoter driven GFP plasmid (cytoplasm marker). Bars = 10 μ m.

3.3. Melatonin-mediated MPK3/6 activation and defense gene induction.

Melatonin activates mitogen-activated protein kinase3/6 (MPK3/6) and induces a number of defense genes leading to stress tolerance in plants (9). To investigate whether melatonin-mediated responses are blocked in the *cand2* mutants, *Arabidopsis* leaves were treated with melatonin (1 μ M). MPK3/6 was significantly activated upon melatonin treatment in the wild type Col-0 and *cand2-1*, whereas it was slightly reduced in *cand2-2* (Figure 4A). In particular, in the absence of melatonin treatment, MPK3/6 activation increased in the *cand2-2* relative to that in wild type Col-0. These data indicate that activation of MPK3/6 was not abolished even in the *cand2-2* mutants, suggesting that Cand2 had little influence on melatonin-mediated mitogen-activated protein kinase (MAPK) activation. Consistent with the MPK3/6 activation, the induction of defense genes upon melatonin treatment, such as luminal binding protein 2 (*BIP2*), ascorbate peroxidase 1 (*APX1*), and glutathione S-transferase 1 (*GST1*), was nearly identical between Col-0 and the *cand2* mutants (Figure 4B). These data clearly suggest that Cand2 protein is not functionally associated with melatonin-mediated defense gene induction, which is dependent on MAPK activation (9).

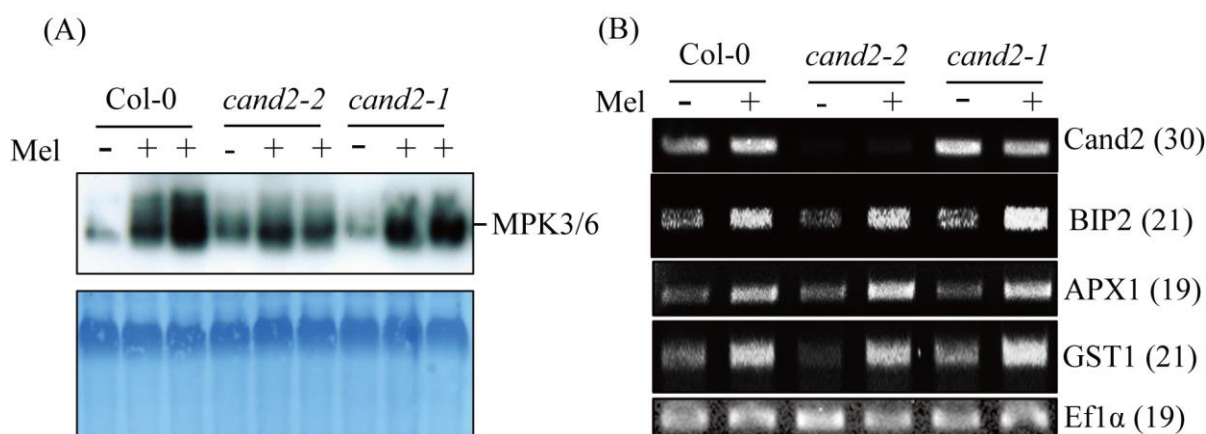


Fig. 4. Activation of MPK3/6 in wild type Col-0, *cand2-1*, and *cand2-2* in response to exogenous melatonin treatment.

(A) Activation of MPK3/6 in wild type Col-0, *cand2-1*, and *cand2-2* in response to melatonin treatment (1 μ M). The lower panel shows Coomassie blue staining of the proteins. (B) Expression levels of ER chaperone and ROS defense genes in wild type Col-0, *cand2-1*, and *cand2-2* in response to melatonin treatment (1 μ M). The induction of BIP2, APX1, and GST1 was measured at 3 h after melatonin treatment. Wild-type *Arabidopsis* Col-0 and two knockout lines were treated with 1 μ M of melatonin for 10 min. Here, + denotes two replications of the same melatonin treatment. Protein extracts from the leaf tissues were analyzed by immunoblotting using an α -pTEpY antibody. Equal loading of proteins was shown by Coomassie blue staining. Numbers in parentheses are the numbers of PCR cycles. BIP2, luminal binding protein 2; APX1, ascorbate peroxidase 1; GST1, glutathione S-transferase 1; Efl α , EFlALPHA; MPK3/6, mitogen-activated protein kinase 3/6.

3.4. ER stress response in the *cand2* mutant.

Melatonin is positively involved with endoplasmic reticulum (ER) stress tolerance through the induction of several ER chaperone genes, including BIP2/3 and calnexin (*CNX1*), via the MAPK signaling cascade (7). If Cand2 were functionally linked with melatonin perception and the melatonin-mediated defense response, melatonin-mediated ER stress tolerance would be expected to be abolished in the *cand2* mutants. To investigate this,

Arabidopsis leaves were treated with Tm, and the induction of ER stress-related genes was examined. Several ER defense genes were greatly induced in both Col-0 and the *cand2* mutants in response to Tm (Figure 5A). Additionally, ion leakage analysis indicated that the *cand2* mutants were not more susceptible than the wild type Col-0 following Tm treatment, which was consistent with the defense gene induction results (Figure 5B). Furthermore, superoxide levels did not differ between Col-0 and the *cand2* mutants. These data clearly suggest that Cand2 is not involved with the melatonin-mediated ER defense response in *Arabidopsis*.

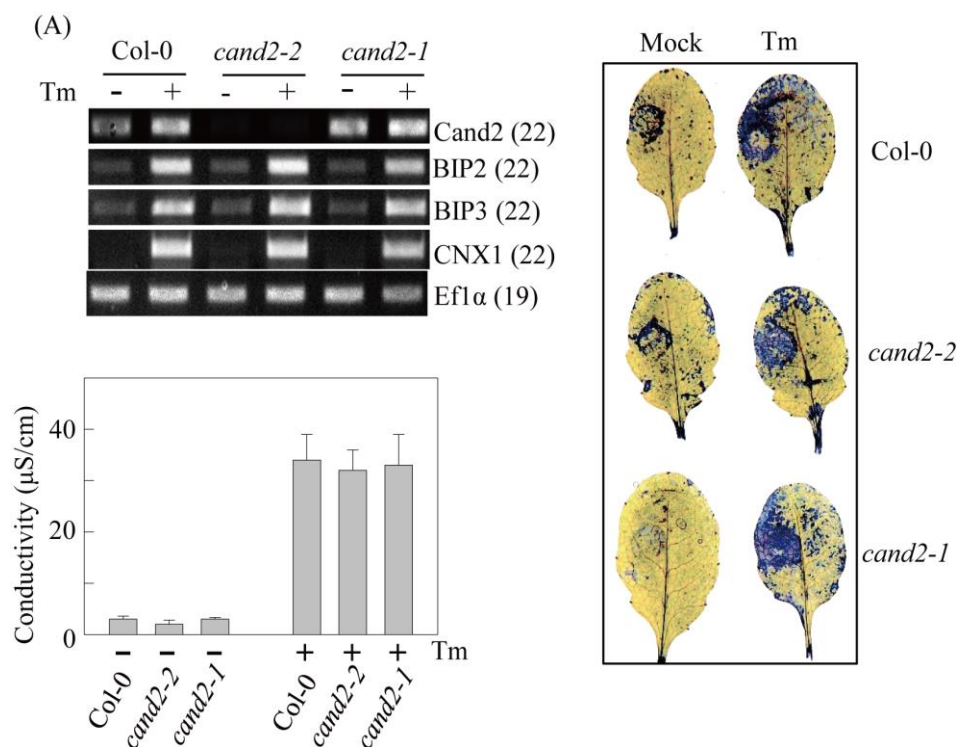


Fig. 5. Induction of defense genes in response to tunicamycin (Tm) treatment.

(A) Transcriptional activation of ER chaperon genes in Col-0 and two *cand2* lines in response to Tm. (B) Ion leakage analysis of Col-0 and two *cand2* lines in response to Tm. (C) Superoxide level of wild type Col-0 and two *cand2* lines in response to Tm. Five-week-old *Arabidopsis* leaves were syringe-infiltrated with a solution containing 1 μg/mL of Tm or 0.05% DMSO (-) (mock) and incubated for 5 h before nitro blue tetrazolium (NBT) staining and RNA analysis. For ion leakage analysis, excised leaves were washed briefly and then incubated with 20 mL of water for 10 h. Numbers in parentheses are the numbers of PCR cycles. BIP2, luminal binding protein 2; BIP3, luminal binding protein 3; CNX1, calnexin1; Eflα, EF1ALPHA.

3.5. Melatonin-mediated MAPK activation and defense gene induction in G-protein mutants.

G proteins are essential components of the GPCR signaling pathway. We investigated whether mutants (*gpa1* and *agb1*) of two of the three G protein subunits (Gα and Gβ, respectively) were associated with melatonin-triggered MAPK activation and defense gene induction. Three defense genes, *BIP2*, *GST1*, and *APX1*, were monitored in response to melatonin treatment. These three defense genes were equally induced in the Col-0, *gpa1*, and *agb1*, suggesting that G protein signaling is irrelevant in melatonin-triggered defense gene induction (Figure 6A). Additionally, melatonin-mediated MPK3 and MPK6 activation was

not hindered in these G protein mutants. Collectively, melatonin-triggered physiological functions are independent of the GPCR signaling pathway.

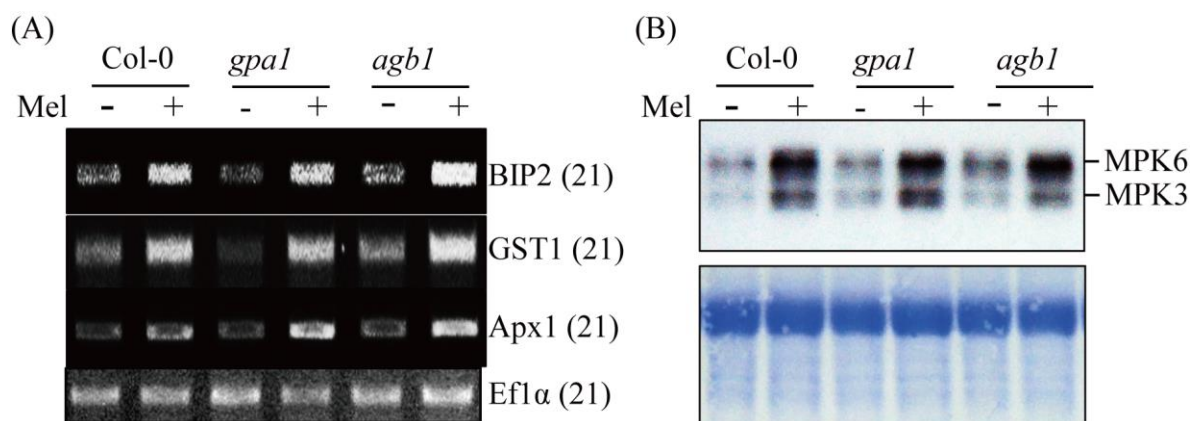


Fig. 6. Melatonin-mediated defense gene induction in G protein–signaling mutants *gpa1* (G α) and *agb1* (G β).

(A) ER chaperone and ROS defense gene expression in wild type *Col-0*, *gpa1*, and *agb1* knockout lines in response to melatonin treatment (1 μ M). (B) MPK3/6 activation in wild type *Col-0*, *gpa1*, and *agb1* knockout lines in response to melatonin treatment (1 μ M). The lower panel presents Coomassie blue staining of the proteins, revealing predominant expression of the Rubisco large subunit. Leaf tissues from five-week-old *Arabidopsis* plants were treated with melatonin (1 μ M) for 10 min, followed by protein immunoblotting as described in Figure 4. Numbers in parentheses are the numbers of PCR cycles. BIP2, luminal binding protein 2; GST1, glutathione S-transferase 1; APX1, ascorbate peroxidase 1; EFL1 α , EFL1ALPHA; MPK3/6, mitogen-activated protein kinase 3/6.

4. CONCLUSION

Identification of a melatonin receptor in plants has long been a primary goal among plant biologists interested in melatonin research. Surprisingly, Wei et al. (6) proposed that Cand2 was a melatonin receptor in plants. Cand2 has a seven-transmembrane-spanning domain, which is one of the conserved features of GPCRs. More importantly, however, GPCRs must also exhibit guanine nucleotide exchange factor (GEF) activity. Based on sequence homology with known GPCRs, *Arabidopsis* GCR1 was the only candidate for plant GPCR, but its status as a GPCR with GEF activity remains uncertain (5). Additionally, Cand2 protein has no sequence homology with GPCRs, thus placing it into a non-GPCR protein family. Apart from the lack of sequence homology between Cand2 and GPCRs, the key subunit of the G protein complex, G α , exists as a GTP-bound active form in plants, meaning that no GPCR is needed to activate it.

In this report, we clearly demonstrate that Cand2 is not involved in melatonin-triggered defense gene induction (Figures 4 and 6), nor is Cand2 located in the plasma membrane (Figures 2 and 3). Additionally, the downstream G α and G β subunits are not associated with the melatonin signaling pathway (Figure 6). Similarly, melatonin-mediated MPK3/6 activation was not hindered in the *cand2-1* mutant but was slightly inhibited in the *cand2-2* mutant. Of note, MPK3/6 levels were slightly higher in the *cand2-2* mutant in the absence of melatonin treatment, for reasons that remain unknown.

Melatonin is a well-known biomolecule that plays significant roles in plants and animals (2, 10–12). Its potent antioxidant activity has been well conserved in all organisms studied to date (2, 13), although its other biological functions and metabolisms have diverged

greatly among organisms, especially between plants and animals (13–17). Further in-depth study of its signaling pathway, including identification of a melatonin receptor, will help clarify the mechanisms underlying how melatonin is associated with a wide range of physiological activities in plants.

ACKNOWLEDGMENTS

This research was supported by grants from the Next-Generation BioGreen 21 Program (SSAC Project No. PJ01325501) and the Research Fellow Program of the National Research Foundation of Korea (NRF-2017R1A6A3A11028333) funded by the Ministry of Education, Republic of Korea.

AUTHORSHIP

H.Y. Lee designed and carried out the experiments and K. Back advised and wrote the article.

CONFLICT OF INTERESTS

The authors declare that there are no conflicts of interest.

REFERENCES

1. Zhao D, Yu Y, Shen Y, Liu Q, Zhao Z, Sharma R, Reiter RJ (2019) Melatonin synthesis and function: evolutionary history in animals and plants. *Front. Endocrinol.* **10**: 249.
2. Tan D-X, Reiter RJ (2019) Mitochondria: the birth place, battle ground and site of melatonin metabolism in cells. *Melatonin Res.* **2** (1): 44-66.
3. de Mendoza A, Sebé-Pedrós A, Ruiz-Trillo I (2014). The evolution of the DPCR signaling system in eukaryotes: modularity, conservation, and the transition to metazoan multicellularity. *Genome Biol. Evol.* **6**: 606-619.
4. Urano D, Chen JG, Botella JR, Jones AM (2013) Heterotrimeric G protein signaling in the plant kingdom. *Open Biol.* **3**: 120186.
5. Urano D, Jones AM (2013) “Round up the usual suspects”: a comment on nonexistent plant G protein-coupled receptors. *Plant Physiol.* **161**: 1097-1102.
6. Wei J, Li DX, Zhang JR, Shan C, Rengel Z, Song ZB, Chen Q (2018) Phytomelatonin receptor PMTR1-mediated signaling regulates stomatal closure in *Arabidopsis thaliana*. *J. Pineal Res.* **65**: e12500.
7. Lee HY, Back K. (2016) Mitogen-activated protein kinase pathways are required for melatonin-mediated defense responses in plants. *J. Pineal Res.* **60**: 327-335.
8. Lee HY, Back K (2018) Melatonin plays a pivotal role in conferring tolerance against endoplasmic reticulum stress via mitogen-activated protein kinases and bZIP60 in *Arabidopsis thaliana*. *Melatonin Res.* **1**: 93-107.
9. Chinchilla, D, Bauer Z, Regenass M, Boller T, Felix G. (2006) The *Arabidopsis* receptor kinase FLS2 binds flg22 and determines the specificity of flagellin perception. *Plant Cell* **18**: 465-476.
10. Arnao MB, Hernández-Ruiz J (2019) Melatonin and reactive oxygen and nitrogen species: a model for the plant redox network. *Melatonin Res.* **2** (3): 152-168.
11. Hardeland R (2019) Melatonin in the evolution of plants and other phototrophs. *Melatonin Res.* **2** (3): 10-36.
12. Pal PK, Bhattacharjee B, Chattopadhyay A, Bandyopadhyay D. (2019) Pleiotropic roles

- of melatonin against oxidative stress mediated tissue injury in the gastrointestinal tract: An overview. *Melatonin Res.* **2** (2): 158-184.
13. Arnao MB, Hernández-Ruiz J (2019b) Melatonin as a chemical substance or as phytomelatonin rich-extracts for use as plant protector and/or biostimulant in accordance with EC legislation. *Agronomy* **9**, 570.
 14. Choi GH, Back K (2019) Cyclic 3-hydroxymelatonin exhibits diurnal rhythm and cyclic 3-hydroxymelatonin overproduction increases secondary tillers in rice by upregulating *MOCI* expression. *Melatonin Res.* **2** (3): 120-138.
 15. Yu Y, Lv Y, Shi Y, Li T, Chen Y, Zhao D, Zhao Z (2018) The role of phyto-melatonin and related metabolites in response to stress. *Molecules* **23**: 1887.
 16. Lee K, Hwang OJ, Back K. (2020) Rice *N*-acetylserotonin deacetylase regulates melatonin levels in transgenic rice. *Melatonin Res.* **3** (1): 32-42.
 17. Galano A, Reiter RJ. (2018) Melatonin and its metabolites vs oxidative stress: From individual actions to collective protection. *J. Pineal Res.* **65**: e12514.



This work is licensed under a [Creative Commons Attribution 4.0 International License](https://creativecommons.org/licenses/by/4.0/)

Please cite this paper as:

Lee, H.Y. and Back, K. 2020. The phytomelatonin receptor (PMRT1) *Arabidopsis* Cand2 is not a bona fide G protein-coupled melatonin receptor. *Melatonin Research.* **3**, 2 (Jun. 2020), 176-186. DOI:<https://doi.org/10.32794/mr11250055>.